Finite-dimensional Optimal Control of Poiseuille Flow

Sanjay S. Joshi*
JPL, California Institute of Technology, Pasadena, California 91109

Jason L. Speyer† and John Kim‡
UCLA, Los Angeles, California 90095

September 3, 1998

Abstract

In this paper, we consider linear stabilization of plane, **Poiseuille flow** using linear quadratic Gaussian optimal control theory. It is shown that we may significantly increase the dissipation rate of perturbation energy, while reducing the required control energy, as compared to that reported using simple, integral compensator control schemes. Poiseuille flow is described by the infinite-dimensional Navier-Stokes equations. Since it is impossible to implement infinite-dimensional controllers, we implement high, but finite-order controllers. We show that this procedure can in theory lead to destabilization of unmodeled dynamics. We then show that this may be avoided using distributed control or, dually, distributed sensing. A problem in high plant order linear quadratic Gaussian controller design is numerical instability in the synthesis equations. We show a linear quadratic Gaussian design that uses an extremely low-order plant model. This low-order controller produces results essentially equivalent to the high-order controller.

flow control
infinite dimensional systems

*MS198-326, JPL, 4800 Oak Grove Drive, Pasadena, CA 91109. Member AIAA.

†38-137 Engineering IV, Department of Mechanical and Aerospace Engineering, UCLA, Los Angeles, CA 90095. Fellow AIAA.

‡48-121 Engineering IV, Department of Mechanical and Aerospace Engineering, UCLA, Los Angeles, CA 90095. Associate Fellow AIAA.

Nomenclature

A, B, C, D = state space representation of system
E_u = control energy
H = channel half-height
$J(u)$ = cost functional
$K_e, \overline{K_e}$ = estimator gain
L = non-dimensional channel length
$P, \overline{P}$ = solution of controller Riccati equation
$P_e, \overline{P_e}$ = covariance of estimator error
$\widehat{p}(x, y, t)$ = small perturbation of pressure
$P^*(x, y, t)$ = primary pressure field solution
Q_e, W_e = power spectral density matrices of process and measurement noises
R, Λ = state and control weighting matrices
$Re = U_c H/\nu$, Reynold's number
s = complex frequency
$\widehat{u}(x, y, t), \widehat{v}(x, y, t)$ = small perturbation of flow velocity in x and y directions
$U^*(y)$ = primary Poiseuille flow solution for velocity in x direction
U_c = centerline velocity
$V^*(x, y, t)$ = primary velocity of flow in y direction
$u(t)$ = scalar input function
$v(t), w(t)$ = Gaussian, white process and measurement noises
x, y = channel coordinates in streamwise and wall-normal directions
z = streamwise component of shear
α = wavenumber
ν = kinematic viscosity
ψ = stream function
γ = degree of closed-loop stability
$()_u, ()_m$ = unmodeled and modeled components
$[a(x), b(x)]_x$ = inner product of a and b defined as $1/L \int_{-L/2}^{L/2} a(x)b(x)dx$
$|.|$ = absolute value
$\triangleq$ = defined as

1 Introduction

The basic concepts of feedback control of plane, Poiseuille flow were laid out in Joshi et. al. [2]. It was shown that the governing Navier-Stokes equations can be converted to control-theoretic transfer function and state space models using a numerical discretization method.

Using the transfer function models, it was shown that plane Poiseuille flow (channel flow) can be stabilized using a simple, constant gain feedback, integral compensator controller. By choosing proper sensor locations, Joshi, et. al. [2] were able to achieve a stable, closed-loop system that was extremely robust to changing Reynolds numbers. The subject of this paper is the description of an optimal controller by moving away from classical transfer function control design to state space methods. In the transfer function design used thus far, the system was stabilized, but the stable system still had closed-loop eigenvalues very near the imaginary s-axis. This resulted in slow dissipation of perturbation energy. The present design provides an optimal, stabilizing controller that achieves a significantly faster dissipation rate of perturbation energy, while reducing required control energy.

Unlike the simple integral feedback control of Joshi, et. al. [2], optimal controllers are complicated systems in themselves [1]. This adds considerably to the complexity of the overall closed-loop system. In fact, many beneficial qualities have been proven only when the controller is of the same dimension as that of the plant. In the flow case, this brings a special problem since the plant is of infinite dimension. Theoretically, the controller must also be of infinite dimension. This is impractical for many reasons. First, it is impossible to physically implement an infinite-dimensional controller. Secondly, the use of even very high-order finite-dimensional plants for controller design leads to numerical problems in the optimal control synthesis equations. We will design an optimal controller using a finite-order model of the infinite-dimensional plant. However, applying reduced order controllers to full order plants has the risk of making unmodeled, stable parts of the plant unstable. Therefore, controllers must be designed to ensure this does not happen.

This paper is organized as follows. In section 2, the linear channel flow problem, state-variable control models, and the single-wavenumber flow model are reviewed. This section is essentially a review of that contained in Joshi, et. al. [2]. In sections 3 and 4, a LQG controller design is introduced and ways in which closed-loop eigenvalues can be made stable to a prescribed degree are shown. Section 5 explains how the unavoidable unmodeled dynamics of any reduced order model of an infinite-dimensional plant can lead to closed-loop instability in LQG design. Distributed actuation and distributed sensing are shown to be dual solutions to the stability problem. Section 6 demonstrates the performance of high-order optimal controllers. Finally, section 7 presents an extremely low-order controller design that achieves comparable performance to the high-order optimal controller design.

2 The Linear Channel Flow Control Problem

2.1 Dynamic Equations

We consider the same plant as in Joshi, et. al. [2], i.e. two-dimensional, plane, Poiseuille flow between two parallel, stationary plates. Let the channel be of finite length and finite

height, with the centerline at zero. The flow in the channel is described by the Navier-Stokes equations. Poiseuille flow is an exact solution to the non-linear, incompressible Navier-Stokes equations given flow driven by an externally imposed pressure gradient through two stationary walls. It is given as $U^*(x,y,t) = U^*(y) = 1-y^2$, $V^*(x,y,t) = 0$, and $P^*(x,y,t) = -2x/Re$. Given the primary Poiseuille flow, consider small perturbations in the velocities of $\widehat{u}(x,y,t)$ in the horizontal direction, $\widehat{v}(x,y,t)$ in the vertical direction, and $\widehat{p}(x,y,t)$ in the pressure field. The linearized, incompressible Navier-Stokes equations may be formed by substituting the primary flow and small perturbations into the non-linear, incompressible Navier-Stokes equations and disregarding the second-order terms involving the perturbations,

$$\frac{\partial \widehat{u}(x,y,t)}{\partial t} + U(y)\frac{\partial \widehat{u}(x,y,t)}{\partial x} + \frac{dU(y)}{dy}\widehat{v}(x,y,t) = -\frac{\partial \widehat{p}(x,y,t)}{\partial x} + \frac{1}{Re}\bigtriangledown^2 \widehat{u}(x,y,t) \quad (1)$$

$$\frac{\partial \widehat{v}(x,y,t)}{\partial t} + U(y)\frac{\partial \widehat{v}(x,y,t)}{\partial x} = -\frac{\partial \widehat{p}(x,y,t)}{\partial y} + \frac{1}{Re}\bigtriangledown^2 \widehat{v}(x,y,t) \quad (2)$$

$$\frac{\partial \widehat{u}(x,y,t)}{\partial x} + \frac{\partial \widehat{v}(x,y,t)}{\partial y} = 0 \quad (3)$$

where the flow variables are non-dimensionalized by the channel half-height,H, and centerline velocity, U_c. By introducing a "stream function", $\psi(x,y,t)$, where

$$\widehat{u}(x,y,t) \triangleq \frac{\partial \psi(x,y,t)}{\partial y} \quad (4)$$

and

$$\widehat{v}(x,y,t) \triangleq -\frac{\partial \psi(x,y,t)}{\partial x} \quad (5)$$

(1- 3) may be combined into a single equation,

$$\frac{\partial}{\partial t}\frac{\partial^2 \psi}{\partial x^2} + \frac{\partial}{\partial t}\frac{\partial^2 \psi}{\partial y^2} = -U(y)\frac{\partial^3 \psi}{\partial x^3} - U(y)\frac{\partial}{\partial x}\frac{\partial^2 \psi}{\partial y^2} + \frac{d^2U(y)}{dy^2}\frac{\partial \psi}{\partial x} + \frac{1}{Re}\bigtriangledown^2\left(\bigtriangledown^2 \psi\right) \quad (6)$$

Assume periodic boundary conditions in the streamwise (x) direction. For channel flow, with rigid plates at $y=-1$ and $y=1$, the no-slip boundary conditions become,

$$\psi(x, y=-1, t) = 0 \quad (7)$$

$$\frac{\partial \psi}{\partial y}(x, y=-1, t) = 0 \quad (8)$$

$$\psi(x, y=1, t) = 0 \quad (9)$$

$$\frac{\partial \psi}{\partial y}(x, y=1, t) = 0 \quad (10)$$

With an initial condition,

$$\psi(x, y, t = 0) = g(x, y) \tag{11}$$

the boundary value problem is completely formed. Equations (6-11) represent the starting point for construction of a feedback control system. These equations neither include any control terms nor do they describe any sensing of flow field variables.

2.2 Boundary Input

We consider the case of blowing/suction at the lower wall of the channel. The boundary conditions are now modified from before to include boundary input, represented as the *known* separable function $q(t)l(x)f(y)$,

$$\psi(x, y = -1, t) = q(t)l(x)f(y = -1) \tag{12}$$

$$\frac{\partial \psi}{\partial y}(x, y = -1, t) = q(t)l(x)\frac{\partial f(y = -1)}{\partial y} = 0 \tag{13}$$

$$\psi(x, y = 1, t) = 0 \tag{14}$$

$$\frac{\partial \psi}{\partial y}(x, y = 1, t) = q(t)l(x)\frac{\partial f(y = 1)}{\partial y} = 0 \tag{15}$$

Note that these conditions constrain the function $f(y)$ such that $f(y = -1) \neq 0$, $\frac{\partial f(y=-1)}{\partial y} = 0$, $f(y = 1) = 0$, and $\frac{\partial f(y=1)}{\partial y} = 0$. Many functions may be appropriate. One such function is

$$f(y) = \frac{1}{2}y^4 + \frac{1}{4}y^3 - y^2 - \frac{3}{4}y + 1 \tag{16}$$

In order to relate boundary conditions on ψ to blowing/suction in the wall-normal direction, we use (5) to relate $\hat{v}(x, y, t)$ and $\psi(x, y, t)$. Then (12) becomes

$$\hat{v}(x, y = -1, t) = -q(t)\frac{\partial l(x)}{\partial x}f(y = -1) \tag{17}$$

Note that $\hat{v}(x, y, t)$ is related to the *derivative* of $l(x)$.

The homogeneous equation (6) and the inhomogeneous boundary condition (12) can be converted into an inhomogeneous equation with homogeneous boundary conditions by introducing

$$\phi(x, y, t) \triangleq \psi(x, y, t) - q(t)f(y)l(x) \tag{18}$$

Then by substituting (18) into (6), we obtain

$$\frac{\partial}{\partial t}\frac{\partial^2 \phi}{\partial x^2} + \frac{\partial}{\partial t}\frac{\partial^2 \phi}{\partial y^2} = -U(y)\frac{\partial^3 \phi}{\partial x^3} - U(y)\frac{\partial}{\partial x}\frac{\partial^2 \phi}{\partial y^2} + \frac{d^2U(y)}{dy^2}\frac{\partial \phi}{\partial x} + \frac{1}{Re}\frac{\partial^4 \phi}{\partial x^4} + 2\frac{1}{Re}\frac{\partial^2}{\partial x^2}\frac{\partial^2 \phi}{\partial y^2} + \frac{1}{Re}\frac{\partial^4 \phi}{\partial y^4} -$$

$$\frac{\partial q(t)}{\partial t}\frac{\partial^2 l(x)}{\partial x^2}f(y) - \frac{\partial q(t)}{\partial t}l(x)\frac{\partial^2 f(y)}{\partial y^2} - q(t)\frac{\partial^3 l(x)}{\partial x^3}U(y)f(y) - q(t)\frac{\partial l(x)}{\partial x}U(y)\frac{\partial^2 f(y)}{\partial y^2} +$$
$$q(t)\frac{\partial l(x)}{\partial x}\frac{d^2U(y)}{dy^2}f(y) + \frac{1}{Re}q(t)\frac{\partial^4 l(x)}{\partial x^4}f(y) + 2\frac{1}{Re}q(t)\frac{\partial^2 l(x)}{\partial x^2}\frac{\partial^2 f(y)}{\partial y^2} + \frac{1}{Re}q(t)l(x)\frac{\partial^4 f(y)}{\partial y^4} \quad (19)$$

The boundary conditions in terms of ϕ are now $\phi(y=-1)=0$, $\frac{\partial\phi(y=-1)}{\partial y}=0$, $\phi(y=1)=0$, and $\frac{\partial\phi(y=1)}{\partial y}=0$. The first line of (19) is the original dynamical equation, (6), and the next two lines are all known input terms.

2.3 Boundary Output

We use the streamwise component of shear at a single boundary point, $z(x_i, y=-1, t)$, as our boundary output, which is given by $z(x_i, y=-1, t) = \frac{\partial\widehat{u}(x_i, y=-1, t)}{\partial y}$. By expressing $\widehat{u}(x_i, y=-1, t)$ in terms of the stream function (4), $z(x_i, y=-1, t) = \frac{\partial^2\psi(x_i, y=-1, t)}{\partial y^2}$ and by observing (18)

$$z(x_i, y=-1, t) = \frac{\partial^2\psi(x_i, y=-1, t)}{\partial y^2} = \frac{\partial^2\phi(x_i, y=-1, t)}{\partial y^2} + q(t)\frac{\partial^2 f(y=-1)}{\partial y^2}l(x_i) \quad (20)$$

2.4 State-Space Formulation

As described in Joshi, et. al. [2], the linear partial-differential flow equation (19) can be converted to a set of linear ordinary-differential equations by use of a Galerkin method. Approximate the solution of (19) as

$$\phi(x, y, t) = \sum_{n=-N}^{N}\sum_{m=0}^{M} a_{nm}(t)P_n(x)\Gamma_m(y) \quad (21)$$

and then use appropriate inner products to obtain a first-order system of equations [4]. In (21), $\Gamma_m(y)$ are formed from Chebyshev polynomials [4] and

$$P_n(x) \triangleq e^{in\alpha_0 x} \quad \alpha_0 = 2\pi/L, -L/2 \le x \le L/2 \quad (22)$$

where the value $(n\alpha_0)$ is called the wavenumber, α, of the system, while α_0 is called the fundamental wavenumber. Note that only integral multiples of the fundamental wavenumber are represented in the solution (21). This comes about since periodic boundary conditions in the x direction can only be satisfied by integral numbers of the fundamental wavenumber.

The resulting ordinary differential equations are then expressed in state-space form by defining the state as a a vector of coefficients, $a_{nm}(t)$ from (21). The result is the standard state space representation,

$$\frac{dx(t)}{dt} = Ax(t) + Bu(t) \quad (23)$$

$$z(t) = Cx(t) + Du(t) \tag{24}$$

In our case, $D = 0$.

2.5 Single Wavenumber Model

We consider the periodic channel model shown in figure 1 with boundary blowing/suction and boundary shear measurement. The Reynolds number considered is $Re = 10,000$. The total length of the channel is $L = 4\pi$ leading to fundamental wavenumber, $\alpha_0 = 0.5$. Recall, only integral multiples of this fundamental wavenumber may exist in the periodic channel. For the single wavenumber model, only one wavenumber is included in the model, corresponding to $\alpha = n\alpha_0 = 1.00$. This wavenumber is selected since it is the only wavenumber that leads to unstable modes for this channel geometry [4]. Input is distributed along the entire bottom plate with a sinusoidal weighting function, $l(x) = sin(x)$. This type of distributed input has very favorable properties. It will be shown in section 5 that a distributed input of this type leads to a system in which all modes are *uncontrollable* except those associated with the wavenumber of $l(x)$. In this case, the wavenumber of, $l(x) = sin(1.0x)$, is $\alpha = 1.0$. Therefore, all modes resulting from all wavenumbers other than 1.0 are uncontrollable. This will allow us to consider only those poles and zeros associated with $\alpha = 1.0$ since the control will affect these modes only. Note that the physical blowing/suction is described by the equation $\hat{v}(x, y, t) = -q(t)\frac{\partial l(x)}{\partial x} f(y = -1) = -q(t)cos(x)f(y = -1)$, (17). The $f(y)$ function in the input is chosen as in (16). In order to visualize the control theoretic model, the A, B, and C matrices of the state space model are transformed to transfer function form. Figure 2 shows the locations of the poles and zeros in the s plane for the channel flow system of figure 1. The numerical verification of these poles and zeros was described in Joshi, et. al. [2].

3 Linear Quadratic Optimal Control Design with Prescribed Degree of Stability

In order to achieve a prescribed degree of stability [5] with an optimal controller, consider the exponential cost functional

$$J(u) \triangleq \lim_{T\to\infty} \frac{1}{T} \int_0^T e^{2\gamma t} \left([Rx(t), x(t)] + [\Lambda u(t), u(t)] \right) dt \tag{25}$$

where the matrix R is semi-positive-definite, Λ is positive-definite and defined a-priori and γ is a positive scalar. We may show [5] that we may convert this problem into a quadratic form and solve for a controller that prescribes all eigenvalues of the closed-loop system to be

to the left of $s = -\gamma$. Rewrite the cost functional as

$$J(u) = \lim_{T\to\infty} \frac{1}{T} \int_0^T [Re^{\gamma t}x(t), e^{\gamma t}x(t)] + [\Lambda e^{\gamma t}u(t), e^{\gamma t}u(t)]dt \tag{26}$$

Define $\overline{x(t)} \triangleq e^{\gamma t}x(t)$ and $\overline{u(t)} \triangleq e^{\gamma t}u(t)$. Then

$$J(\overline{u}) = \lim_{T\to\infty} \frac{1}{T} \int_0^T [R\overline{x}, \overline{x}] + [\Lambda\overline{u}, \overline{u}]dt \tag{27}$$

Note

$$\frac{d\overline{x(t)}}{dt} = \frac{d}{dt}(e^{\gamma t}x(t)) = \gamma e^{\gamma t}x(t) + e^{\gamma t}\frac{dx(t)}{dt} \tag{28}$$

By substituting for $\frac{dx(t)}{dt}$,

$$\frac{d\overline{x}}{dt} = (A + I\gamma)\overline{x} + B\overline{u} \tag{29}$$

Let $\overline{A} \triangleq A + I\gamma$. Then the optimal control is given by $\overline{u_{opt}}(t) = -\Lambda^{-1}B^*\overline{P}\overline{x}(t)$ and

$$u_{opt}(t) = -\Lambda^{-1}B^*\overline{P}x(t) \tag{30}$$

where $\overline{P}$ is obtained by solving the Riccati equation

$$\overline{P}\overline{A} + \overline{A}^*\overline{P} - \overline{P}B\Lambda^{-1}B^*\overline{P} + R = 0 \tag{31}$$

The new closed-loop system dynamics matrix becomes

$$A - B\Lambda^{-1}B^*\overline{P} \tag{32}$$

whose eigenvalues are all to the left of $s = -\gamma$. It can be shown [4] that if (A, B) is controllable and (A, R) is observable, then $(A + \gamma I, B)$ is controllable and there exists a positive definite solution, $\overline{P}$, of the matrix Riccati equation (31) for $R \geq 0$.

In theory, for full-order plant models, there is no restriction on the value of γ. In practice, however, for controllers built using reduced-order plant models, γ is limited by robustness of the controller when applied to the full-order system.

4 Optimal Estimator Design with Prescribed Degree of Stability

In the previous section, we derived an optimal controller. As can be seen from equation (30), the control is always represented in terms of the current state, $x(t)$. These states, however, are not available to us in the channel problem. Instead, we have access to shear

measurements at only one or several locations along the boundary. Therefore, we must construct an observer to estimate the state, $x(t)$, from the measured shear outputs, $z(t)$. In order to see how this is done, consider a noisy version of the state space model shown earlier

$$\frac{dx(t)}{dt} = Ax(t) + Bu(t) + v(t) \tag{33}$$

$$z(t) = Cx(t) + w(t) \tag{34}$$

$$x_0 \triangleq x(t=0) \tag{35}$$

where (A, B) is again assumed controllable and (A, C) is again assumed observable.

Assumption 1 *The noise processes $v(t)$ and $w(t)$ are white, Gaussian, of zero mean, independent of each other, and have known covariances. The matrices P_0, Q_e, and W_e are positive-definite.*

$$E[v(t)v^*(\tau)] = Q_e\delta(t-\tau) \quad E[v(t)] = 0 \tag{36}$$

$$E[w(t)w^*(\tau)] = W_e\delta(t-\tau) \quad E[w(t)] = 0 \tag{37}$$

$$E[x(t_0)] = m \tag{38}$$

$$E([x(t_0) - m][x(t_0) - m]^*) = P_0 \tag{39}$$

where $E(.)$ is an expectation operator.

It may be shown that a steady state estimator may be constructed that minimizes the error covariance between the actual state, $x(t)$, and the estimated state, $\hat{x}(Z_t)$, where $Z_t = \{z(l) : -\infty < l \leq t\}$, i.e. the measurement history,

$$\overset{min}{\hat{x}(Z_t)} \qquad E\left([x(t) - \hat{x}(Z_t)][x(t) - \hat{x}(Z_t)]^*\right) \tag{40}$$

It can be shown that the optimal estimate, in the sense of (40), is given by the conditional expectation $\hat{x}(t) \triangleq \hat{x}(Z_t) = E\left(x(t)/Z_t\right)$, where $E\left(./Z_t\right)$ is the conditional mean operator. In the linear case with Gaussian noises, the structure of the estimator is

$$\frac{d\hat{x}(t)}{dt} = A\hat{x}(t) + Bu(t) + K_e(C\hat{x}(t) - z(t)) \tag{41}$$

where

$$K_e = -P_eC^*W_e^{-1} \tag{42}$$

and P_e is calculated from a matrix Riccati equation

$$P_eA^* + AP_e - P_eC^*W_e^{-1}CP_e + Q_e = 0 \tag{43}$$

Note that the stability of (41) depends on the stability of $(A-P_eC^*W_e^{-1}C)$. The assumptions that $W_e, Q_e > 0$ and (A, C) observable assure $\exists P_e > 0$ such that (43) is satisfied.

By considering a slightly different estimator Riccati equation, we may constrain the closed-loop estimator poles to be stable to a prescribed degree. It can be shown [4] that if (A, C) is observable, then $(A + \gamma I, C)$ is observable and there exists a positive definite solution of the matrix Riccati equation

$$\overline{P_e}(A+\gamma I)^* + (A+\gamma I)\overline{P_e} - \overline{P_e}C^*W_e^{-1}C\overline{P_e} + Q_e = 0 \tag{44}$$

for $Q_e > 0$, where γ is a real, positive scalar. Then all eigenvalues of $(A - \overline{P_e}C^*W_e^{-1}C)$ are all to the left of $s = -\gamma$. The new estimator gain is given as

$$\overline{K_e} = -\overline{P_e}C^*W_e^{-1} \tag{45}$$

4.1 Separation Principle in LQG Control

The goal of linear quadratic Gaussian (LQG) design is to combine the results of deterministic linear quadratic control theory and stochastic estimation theory to form an overall control system. As we have seen, our system equations become stochastic with the addition of noise terms. Therefore, in our controller design, we may no longer minimize a deterministic cost functional. Rather, we now minimize the expected value of the cost functional,

$$E(J) = E\left(\lim_{T\to\infty}\frac{1}{T}\int_0^T [Rx(t), x(t)] + [\Lambda u(t), u(t)]dt\right) \tag{46}$$

where $x(t)$ is now a stochastic process. It can be shown that the optimal control is now expressed in terms of the estimated state, $u_{opt}(t) = -\Lambda^{-1}B^*\overline{P}\hat{x}(t)$. The complete LQG solution is then

$$\frac{dx(t)}{dt} = Ax(t) + Bu(t) + v(t) \qquad plant \tag{47}$$

$$z(t) = Cx(t) + w(t) \qquad observation \tag{48}$$

$$x_0 \triangleq x(t=0) \qquad initial\ \ condition \tag{49}$$

$$\frac{d\hat{x}(t)}{dt} = A\hat{x}(t) + Bu(t) + \overline{K_e}(C\hat{x}(t) - z(t)) \qquad estimator \tag{50}$$

$$u_{opt}(t) = -\Lambda^{-1}B^*\overline{P}\hat{x}(t) \qquad feedback \tag{51}$$

where $\overline{P}$ is the positive-definite solution of (31) and $\overline{K_e}$ is given in (45).

We may show that the overall estimator/controller system is stable by stacking the state, $x(t)$, and the error, $e(t) \triangleq \hat{x} - x$, into one vector and studying the dynamics of the new system.

$$\begin{bmatrix} \frac{dx(t)}{dt} \\ \frac{de(t)}{dt} \end{bmatrix} = \begin{bmatrix} (A - B\Lambda^{-1}B^*\overline{P}) & -B\Lambda^{-1}B^*\overline{P} \\ 0 & (A - \overline{P_e}C^*W_e^{-1}C) \end{bmatrix} \begin{bmatrix} x(t) \\ e(t) \end{bmatrix} + \begin{bmatrix} v(t) \\ -K_e w(t) - v(t) \end{bmatrix} \tag{52}$$

The stability of the system is determined by the eigenvalues of the dynamical matrix. Clearly, the eigenvalues are comprised of the eigenvalues of the closed-loop controller, $(A-B\Lambda^{-1}B^*\overline{P})$ and the eigenvalues of the closed-loop estimator, $(A-\overline{P_e}C^*W_e^{-1}C)$. We have already proven that both of these matrices are stable (under appropriate assumptions). Therefore, the overall control system is stable also. This is known as the separation principle in LQG control.

5 Effects of Unmodeled Wavenumber Dynamics on the LQG Problem

We have already seen that the separation principle in LQG control allows us to show that if the controller and estimator are both stable, then the overall system is stable. We will see in this section that this principle breaks down in the presence of unmodeled dynamics.

Any finite-dimensional model is a reduced-order model for the infinite-dimensional channel flow problem. In terms of poles and zeros studied earlier, more poles and zeros exist in the system than are accounted for in the model and the subsequent controller design. It is easy to imagine that an unmodeled pole could be drawn to the unstable half of the s plane by a reduced-order controller. As a result, even though the designed controller may stabilize the reduced-order plant, it may not stabilize the actual infinite-dimensional plant. Consider the following partition of the state space model with noise terms added

$$\frac{dx}{dt} = \begin{bmatrix} \frac{dx_m}{dt} \\ \frac{dx_u}{dt} \end{bmatrix} = \begin{bmatrix} A_m & 0 \\ 0 & A_u \end{bmatrix} \begin{bmatrix} x_m \\ x_u \end{bmatrix} + \begin{bmatrix} B_m \\ B_u \end{bmatrix} u(t) + \begin{bmatrix} v_m(t) \\ v_u(t) \end{bmatrix} \tag{53}$$

$$z = \begin{bmatrix} C_m & C_u \end{bmatrix} x + w(t) \tag{54}$$

where the subscripts m and u represent the modeled and unmodeled parts of the system. The process noise, v , and the measurement noise,w, are assumed to be Gaussian, independent, zero mean, white noise processes as in (36) and (37). The unmodeled part is meant to denote only the dynamics of wavenumbers left out of the reduced-order model, represented by $(|n| > N)$ in (21). A_u is assumed stable. Both A_u and A_m are of infinite dimension [2]; A_u because of the infinite number of wavenumbers left out of the reduced-order model and A_m because of the infinite number of poles for each of the finite number of modeled wavenumbers, represented by $(m > M)$ in (21).

Since we only know the modeled part of the system, we design an LQG controller/observer based on that part. Minimize the expected value of a cost functional, J,

$$E(J) = E\left(\lim_{T\to\infty} \frac{1}{T}\int_0^T [Rx_m(t), x_m(t)] + [\Lambda u(t), u(t)]dt\right) \tag{55}$$

where R is any semi-positive definite matrix and Λ is any positive definite matrix. The optimal control is of the form

$$u_{opt}(t) = -\Lambda^{-1} B_m^* \overline{P} \hat{x}_m(t) \tag{56}$$

where $\hat{x}_m(t)$ is the estimate of the modeled state and the matrix,$\overline{P}$, is calculated by solving the algebraic Riccati equation

$$A_m^* \overline{P} + \overline{P} A_m - \overline{P} B_m \Lambda^{-1} B_m^* \overline{P} + R = 0 \tag{57}$$

assuming the same assumptions as in (47)-(51) for the modeled parts.

Since we cannot obtain direct measurements of the current state, $x_m(t)$, we construct an observer as described in section 4

$$\frac{d\hat{x}_m(t)}{dt} = A_m \hat{x}_m(t) + B_m u(t) + \overline{K_e}(C_m \hat{x}_m(t) - z(t)) \tag{58}$$

where the estimator gain $\overline{K_e} = -\overline{P_e} C_m^* W_e^{-1}$ requires the solution of another matrix Riccati equation

$$\overline{P_e} A_m^* + A_m \overline{P_e} - \overline{P_e} C_m^* W_e^{-1} C_m \overline{P_e} + Q_e = 0 \tag{59}$$

Define the error between the estimated, modeled state, $\hat{x}_m(t)$, and the actual state, $x_m(t)$, as $e_m(t)$. Then as in [6]

$$\begin{gathered} \frac{de_m(t)}{dt} \triangleq \frac{d\hat{x}_m(t)}{dt} - \frac{dx_m(t)}{dt} = \\ [A_m - \overline{P_e} C_m^* W_e^{-1} C_m] e_m(t) + \overline{P_e} C_m^* W_e^{-1} C_u x_u(t) \\ + \overline{P_e} C_m^* W_e^{-1} w - v_m \end{gathered} \tag{60}$$

where the unmodeled state acts as a forcing term.

In order to study the entire controller/observer system, stack the modeled state, the modeled error, and the unmodeled state and consider the dynamics of the stacked system (61).

$$\begin{bmatrix} \frac{dx_m}{dt} \\ \frac{de_m}{dt} \\ \frac{dx_u}{dt} \end{bmatrix} = \begin{bmatrix} (A_m - B_m \Lambda^{-1} B_m^* \overline{P}) & -B_m \Lambda^{-1} B_m^* \overline{P} & 0 \\ 0 & (A_m - \overline{P_e} C_m^* W_e^{-1} C_m) & \overline{P_e} C_m^* W_e^{-1} C_u \\ -B_u \Lambda^{-1} B_m^* \overline{P} & -B_u \Lambda^{-1} B_m^* \overline{P} & A_u \end{bmatrix} \begin{bmatrix} x_m \\ e_m \\ x_u \end{bmatrix} + \begin{bmatrix} v_m \\ -\overline{K_e} w - v_m \\ v_u \end{bmatrix} \tag{61}$$

From the LQG theory presented in section 3, $(A_m - B_m \Lambda^{-1} B_m^* \overline{P})$ and $(A_m - \overline{P_e} C_m^* W_e^{-1} C_m)$ are stable. However, from (61), the overall system may not be stable due to the unmodeled

actuator influence , B_u, and sensor influence , C_u, matrices. Therefore, we have seen that in the LQG framework, we cannot insure overall stability unless the unmodeled parts of the system are accounted for.

There are two ways to ensure system (61) is stable, assuming $(A_m + B_m K C_m)$ and A_u are stable. One way is to ensure $B_u = 0$, i.e., make sure the unmodeled dynamics are uncontrollable with respect to the actuator. The other way to ensure a stable system is to assure $C_u = 0$, i.e., make sure the unmodeled dynamics are unobservable with respect to the sensor. Controllability and observability for the plane Poiseuille flow problem were introduced in Joshi, et. al. [2]. We now explore how we may achieve these conditions.

5.1 Point Actuation vs. Distributed Actuation

One way to guarantee the overall system (61) is stable is to assure all modes associated with unmodeled wavenumbers are uncontrollable with respect to the input by making $B_u = 0$. In the fully developed channel flow system, this would account for the wavenumbers left out of the reduced-order model. If

$$l(x) \triangleq Real\left(\sum_{n=-N}^{N} e^{in\alpha_0 x}\right) \tag{62}$$

where the n range corresponds to the modeled wavenumbers only, then the projection of $l(x)$ onto unmodeled wavenumbers is zero due to the orthogonality of Fourier components. As a result, $B_u = 0$ and stability of unmodeled dynamics is retained. Note that since $l(x) \neq 0$ for all but a finite number of points in the x direction, this type of scheme is a distributed actuation scheme. Therefore, by moving from a physically easier to implement "point" actuator to a more difficult distributed actuator, we have retained stability of the unmodeled dynamics. Physically, a distributed actuator is obtained by a large number of independently programmable actuators placed along the lower wall. If distributed actuation is infeasible or undesirable, we must look to the dual problem of sensing to gain stability.

5.2 Point Sensing vs. Distributed Sensing

It is seen from (61), that if $B_u \neq 0$, stability may still be maintained if $C_u = 0$. This corresponds to making all unmodeled wavenumber dynamics unobservable with respect to the shear sensor. Placing a single shear sensor at a point along the lower channel wall results in a measurement that includes the effects of all wavenumbers, both modeled and unmodeled. Clearly, $C_u \neq 0$, and stability is not guaranteed. This corresponds to the point forcing case in the dual problem of actuation. By using a distributed sensing scheme, however, we may form a new measurement that includes only the effects of the modeled wavenumbers. This is done by projecting a distributed shear function, $z(x, y = -1, t)$, onto the modeled wavenumbers. The distributed shear function, $z(x, y = -1, t)$ is physically created by measuring the shear

at all points along the lower channel wall. Then a new projected shear measurement, denoted $\tilde{z}(t)$, is defined as

$$\tilde{z}(t) \triangleq Real\left([z(x, y=-1, t), \sum_{n=-N}^{N} e^{in\alpha_0 x}]_x\right) \tag{63}$$

where again the n range corresponds to modeled wavenumbers only. Note that just as in the actuator case, we have implemented a more physically complicated series of sensors in order to achieve overall stability.

There is a subtle difference between making the channel system unmodeled dynamics unobservable as opposed to uncontrollable. By making unmodeled dynamics uncontrollable, linear stability is maintained (under appropriate conditions) since the unmodeled dynamics cannot be affected by the input. By making unmodeled dynamics unobservable, however, linear stability is also maintained (under appropriate conditions), but unmodeled dynamics may be affected by the input. These affected dynamics could produce transients that cause the linear model to become invalid [2].

In terms of modeling, we need not include either unobservable or uncontrollable modes in our plant models. Therefore, distributed actuation or sensing allows models to be created using only a finite number of wavenumbers. Note, however, that even a single wavenumber model contains an infinite number of modes shown by the infinite number of poles extending out into the left hand s plane as shown in figure 2 (see also [4]).

6 Control Design Using Finite Large Order Models

As we have seen in section 5, we may reduce the problem of including an infinite number of wavenumbers in a reduced-order model to a problem of including a finite number of wavenumbers by using distributed actuation or sensing. However, even with a model containing only a finite number of wavenumbers, the problem is still infinite-dimensional because of the infinite number of poles extending into the left hand s plane for *each* wavenumber. Furthermore, we do not know the exact position of poles far into the left hand s plane due to the finite number of basis functions used in the y direction [4]. Still, these poles must be accounted for in the control design. The fact that uncertain poles appear only at higher frequencies in the bandwidth will be advantageous. It will allow a robust controller to be designed that "rolls off" at high frequencies.

For disturbance rejection, it can be shown [5] that high loop gain is preferable. On the other hand, for good output noise suppression, the loop gain should be *low* at all frequencies in which the noise enters [5]. It is generally assumed that noise is most destructive at higher frequencies. As a result, control design focuses on high loop gain at low frequencies where disturbance rejection is most important and low loop gain at high frequencies where noise is more of a problem. Therefore, an ideal controller will cause loop gain to roll-off at high

frequencies.

In addition to noise at high frequencies, the other major problem at high frequencies is unmodeled dynamics. We have already pointed out that there are two types of unmodeled dynamics in the channel flow problem. The first type is unmodeled dynamics of unmodeled wavenumbers. We accounted for these dynamics through distributed control or distributed sensing. The second type is unmodeled dynamics at high frequencies for modeled wavenumbers. This type of unmodeled dynamics has yet to be considered and is common to most infinite dimensional systems. To account for these dynamics, controllers are designed that give low loop gain at the high frequencies of the open-loop controller/plant series where unmodeled dynamics exist in order not to stimulate modes at those frequencies. Roll-off has also been given a more analytic framework by considering multiplicative, unstructured uncertainty [7].

We consider the one wavenumber model shown in figure 1 with $Re = 10,000$. Only $\alpha = 1.0$ is included in the model. All other wavenumbers are uncontrollable due to the distributed input of $l(x) = sin(x)$ as shown in section 5.1. A single point sensor is located at π. The length of the channel is 4π leading to a fundamental wavenumber of $\alpha_0 = \frac{1}{2}$.

We now design an LQG controller and compare closed-loop response to that of the simple, integral controller introduced in [2]. The integral control method is shown in figure 3 and the LQG control method is shown in figure 4. Two criterion will be used in comparing controllers: (1) output (shear) settling time and (2) required control energy. Control energy will be defined as,

$$E_u \triangleq \sqrt{\int_0^T |u(t)|^2 dt} \tag{64}$$

where T is a finite upper bound.

We consider two models in evaluating the resulting LQG controller: one model of order 252 (Validation Model) and the other model of order 140 (Reduced-order Model). Validation Model is constructed by including all poles and zeros to the right of $s = -4$ (refer to figure 2). Reduced-order Model includes all *observable* and *controllable* poles and zeros to the right of $s = -2$ (refer to figure 2). Reduced-order Model was created by using the `minreal` function within the MATLAB Control Toolbox [8] with the parameter value `tol`$= 1e-3$. Table 1 lists all models considered in this study. The `lqr` and `lqe2` functions of the MATLAB Control Toolbox were used to create an LQG controller using Reduced-order Model. The A matrix supplied to each of these MATLAB functions were modified to $(A + I\gamma)$ in order to achieve a prescribed degree of stability as described in sections 3 and 4 . The following parameters were used: $\gamma = .005$, $R = .001C^*C$, $\Lambda = I$, $Q_e = 10BB^*$, $W_e = 1$. The R matrix was chosen to minimize shear in the cost functional (46); the Q_e matrix was originally chosen to recover robustness properties using loop transfer recovery techniques [9]; γ was chosen by trial and error to decrease settling time without increasing control energy; W_e, and Λ were chosen using trial and error. The gain of the integral controller was chosen as, $K_I = .07$.

Figures 5 and 6 show the shear output and blowing/suction input signal for the closed-loop system (Validation Model plus controller) for the same plant initial condition (`ones(252,1)` in `Matlab`). Clearly, using the LQG controller, the channel system has a much shorter settling time. More significantly, this reduced settling time is accompanied by lower control energy. Indeed, for the LQG case, $E_{LQG} = .5809$, while for the integral controller case, $E_{INT} = .8178$. Note that since all values are non-dimensional, it is the comparison of energies that is important, not the actual numbers. Similar results were obtained for other initial conditions, as well as disturbance inputs.

In analyzing the resulting control system, consider figure 4. The optimal control is defined at $K = 1$ with a properly designed LQG controller. Note many poles in Validation Model are either uncontrollable or unobservable as shown by pole/zero cancellations (figure 2). These poles cannot be moved. We concentrate on moving only the observable/controllable poles. Figure 7 shows the root locus of the controller/estimator, designed using Reduced-order Model (order 140), in series with Validation Model (order 252), for gain values, K, varying from 0 to 4. Poles of the closed-loop system achieve the goal of being to the right of $s = -.005$ with gain, $K = 1$. Consequently, settling time is reduced. Finally, figure 8 shows the magnitude response for the open-loop series connection of the LQG controller (using Reduced-order Model) and Validation Model. Note that the loop gain rolls-off at higher frequencies.

7 Control Design Using Low Order Models

Although we achieved our goal in section 6, we designed our LQG controller with a high dimensional plant model (order 140). This may lead to numerical problems if the design were attempted with a new model that contained several wavenumbers as the model would be even larger. As a result, we would like to develop a design that uses an extremely low-order model. Consider the model shown in figure 9 (Low-order Model). This model contains 8 poles and 7 zeros.

A LQG controller is designed using only Low-order Model. The parameters for the design are the same as in section 6. Figure 10 shows the closed-loop output response of Validation Model (order 252) and controller obtained from Low-order Model (figure 9). An almost identical settling time is achieved compared to the controller using Reduced-order Model (order 140). Also, the control energy is only slightly increased to $E_{low-order} = .6131$. Using this design, we have reduced the order of the LQG controller from 140 to 8, while maintaining performance.

8 Conclusion

Linear stabilization of plane, Poiseuille flow using linear quadratic Gaussian optimal control theory has been examined. The infinite-dimensional nature of the problem poses challenges for finite-dimensional control. Distributed actuation and/or sensing methods, as well as loop gain roll-off, can be used to address the inherent unmodeled dynamics of finite-dimensional models of infinite-dimensional systems. Using linear quadratic Gaussian methods, we achieved significantly higher dissipation rates, while using lower control energy, than those reported in integral compensator control schemes. We showed linear quadratic Gaussian designs that used both a high-order and an extremely low-order plant model for control synthesis. The low-order controller produced results essentially equivalent to the high-order controller. In this paper, we have examined linear quadratic Gaussian control methods. Other control approaches exist that are based on worst-case design [10]. The methods discussed in this paper were aimed at reducing settling time and control energy. However, additional criterion such as limiting transient growth will be important in preserving the integrity of a linear model of channel flow and preventing transition of laminar channel flow to turbulent channel flow.

Acknowledgements

The work described in this paper was performed in part at the Jet Propulsion Laboratory, California Institute of Technology, under a contract with the National Aeronautics and Space Administration, and in part at UCLA sponsored by Air Force Office of Scientific Research URI Grant F496920-97-1-0276 and NASA Dryden Grant NCC2-374-PR41.

References

[1] Joshi, S.S., Speyer, J.L., and Kim, J., "Feedback Stabilization of Plane Poiseuille Flow,"*Proceedings of the Conference on Decision and Control*, New Orleans, LA, 1995, pp. 921-927.

[2] Joshi, S.S., Speyer, J.L., and Kim, J., "A Systems Theory Approach to the Feedback Stabilization of Infinitesimal and Finite-amplitude Disturbances in Plane Poiseuille Flow",*Journal of Fluid Mechanics*, Vol. 331, 1997, pp. 157-184.

[3] Doyle, J.K., "Guaranteed Margins for LQG Regulators *IEEE Transactions on Automatic Control*," Vol. AC-23, No. 4, August, 1978, pp. 664-665.

[4] Joshi, S.S., *A Systems Theory Approach to the Control of Plane Poiseuille Flow*, UCLA , Department of Electrical Engineering, Ph.D. Dissertation,1996.

[5] Anderson, B.O. and Moore, J.B., *Optimal Control: Linear Quadratic Methods* Prentice-Hall, 1990, pp. 110-115.

[6] Sesak, J.R., Likins,P. and Coradetti, T., "Flexible Spacecraft Control by Modal Error Sensitivity Suppression," *Journal of Aeronautical Science*, Vol. XXVII, No. 2, April-June, 1979, pp. 131-156.

[7] Doyle, J. and Stein, G., "Multivariable Feedback Design: Concepts for a Classical/Modern Synthesis," *IEEE Transactions on Automatic Control*, Vol. AC-26, 1981, pp. 4-16.

[8] Grace, A., Laub, A.J., Little, J.N., and Thompson, C.M., *Control System Toolbox: For use with MATLAB*, The Math Works, 1992, pp. 2-102,115,116.

[9] Doyle, J. and Stein, G., "Robustness with Observers," *IEEE Transactions on Automatic Control*, Vol. AC-24, No. 4, 1979, pp. 607-611.

[10] Rhee, I. and Speyer, J.L., "A game theoretic approach to a finite-disturbance attenuation problem," *IEEE Transactions on Automatic Control*, Vol. 36, 1991, pp. 1021-1032.

Model Name	**Order**
Validation	252
Reduced-order	140
Low-order	8

Table 1: Models used in LQG controller design.

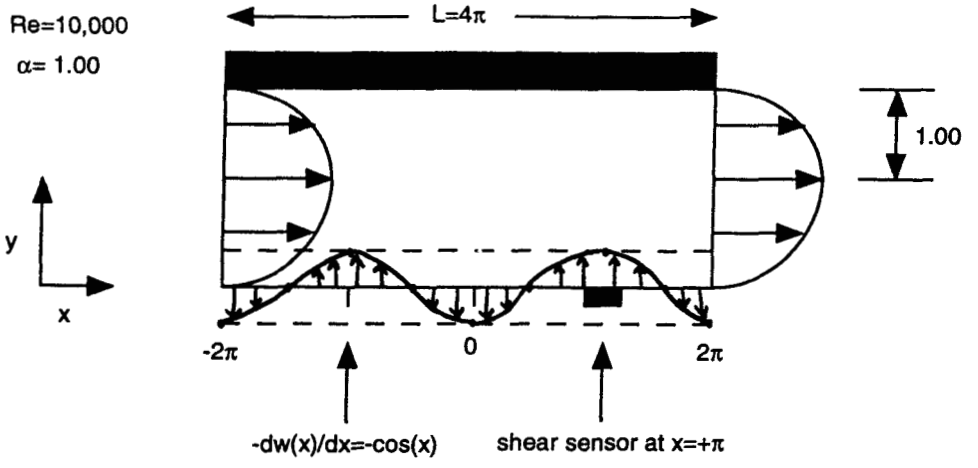

Figure 1: System model for Poiseuille channel flow.

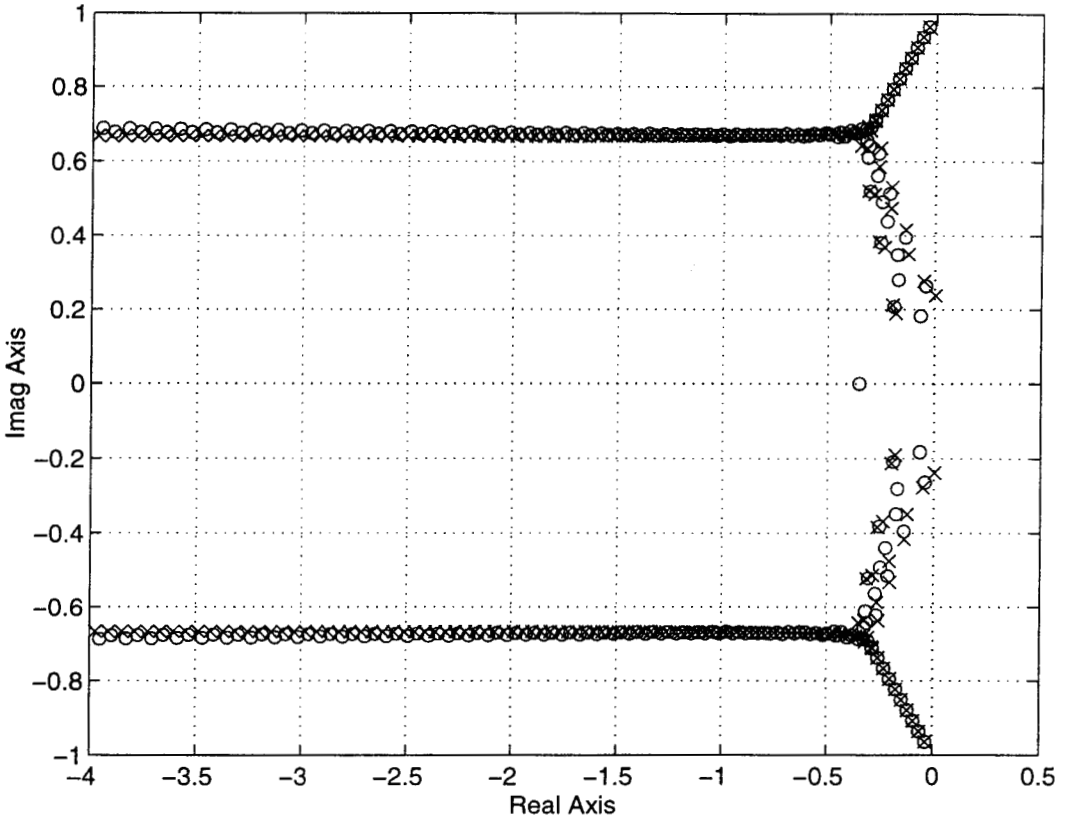

Figure 2: Pole (x) /Zero (o) Configuration, Channel model: $Re = 10,000$, shear sensor at π, $l(x) = sin(x)$,L=4π, $\alpha = 1.0$.

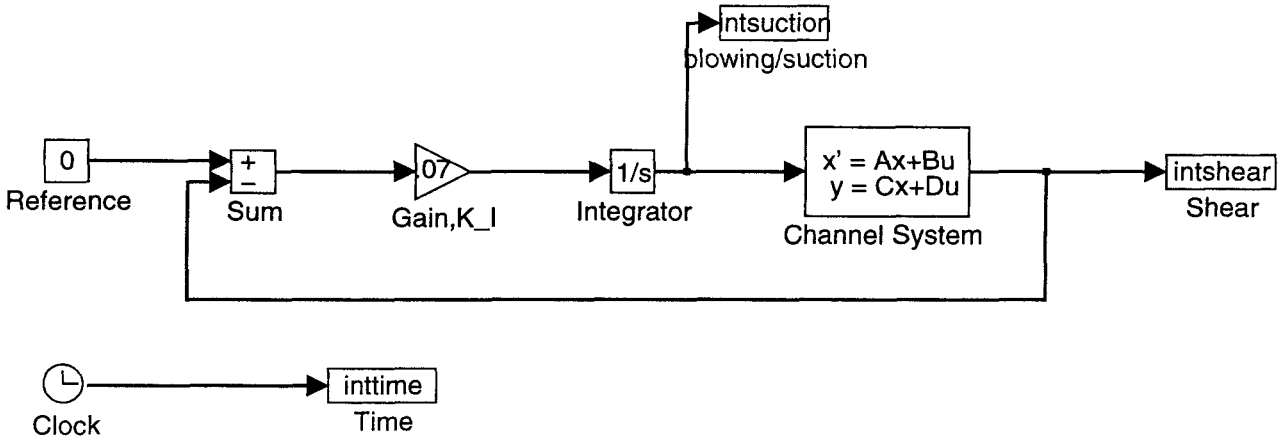

Figure 3: Integral control block diagram.

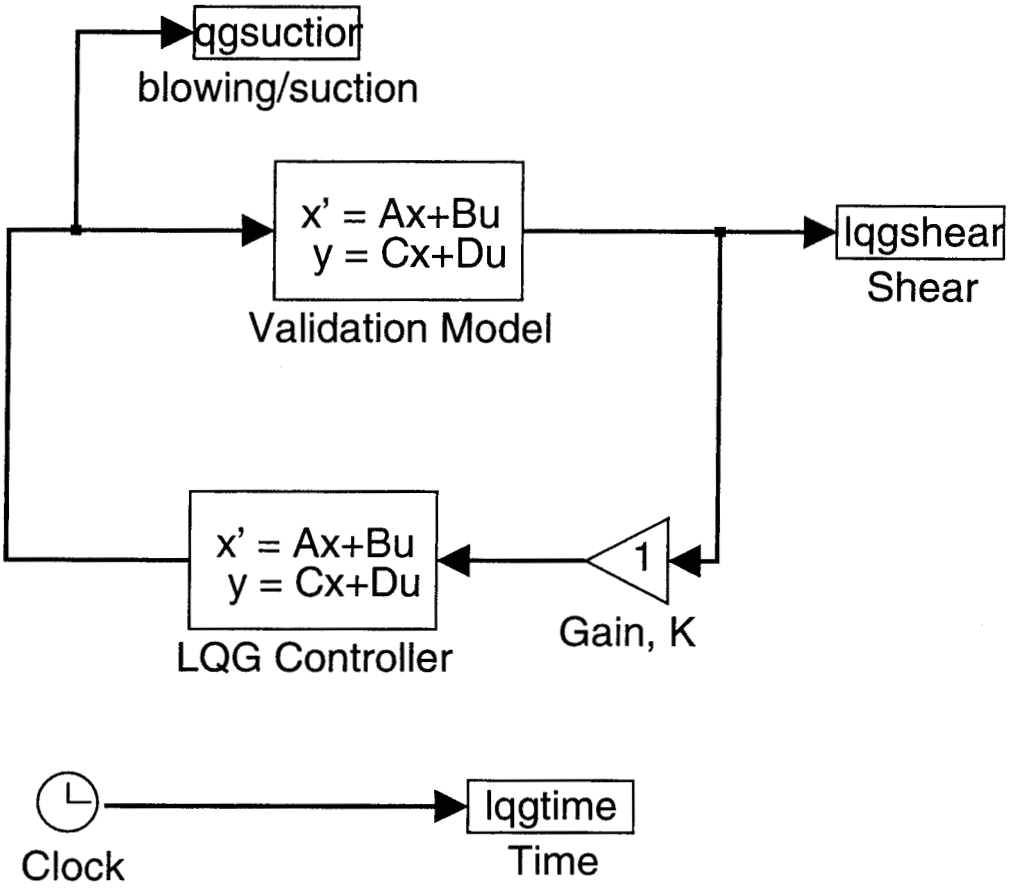

Figure 4: LQG control loop for Validation Model plant and LQG controller.

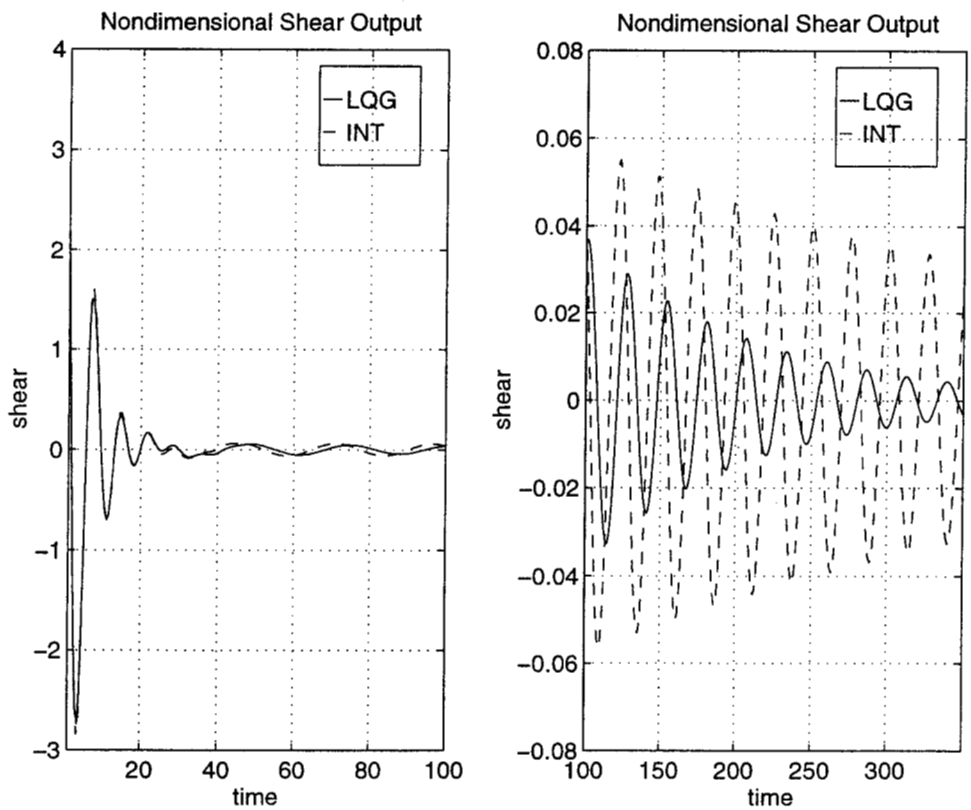

Figure 5: Shear at ouput of closed-loop system. Dashed line is output from integral control method. Solid line is output from reduced-order LQG control method.

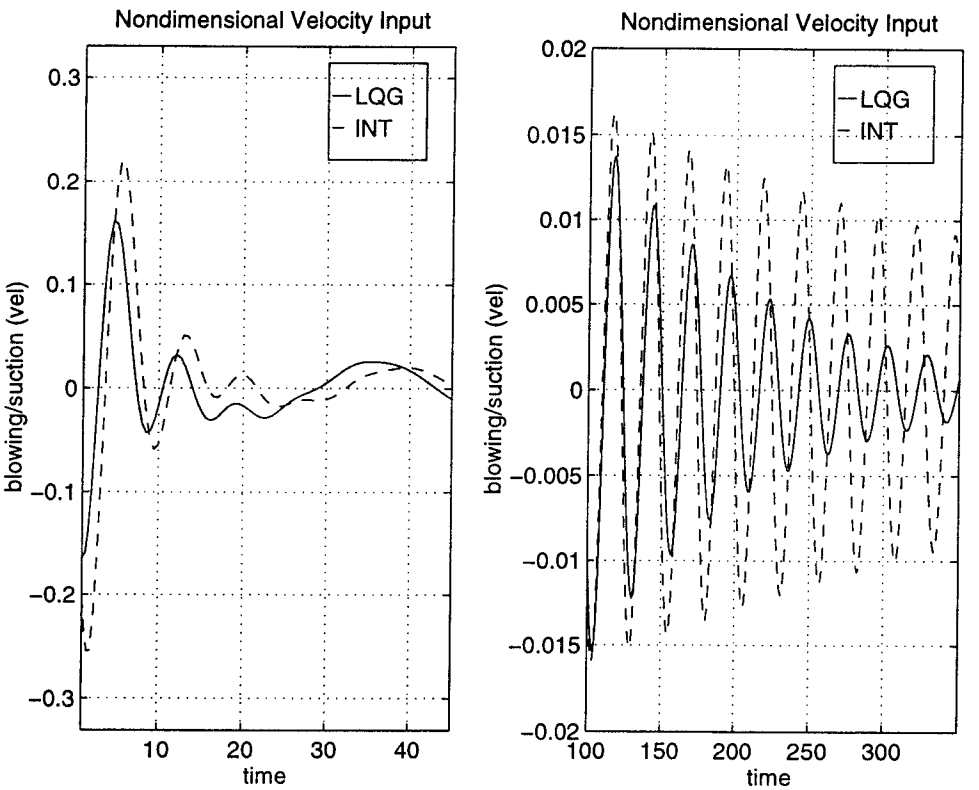

Figure 6: Blowing and suction control input. Dashed line is input from integral control method. Solid line is input from reduced-order LQG control method.

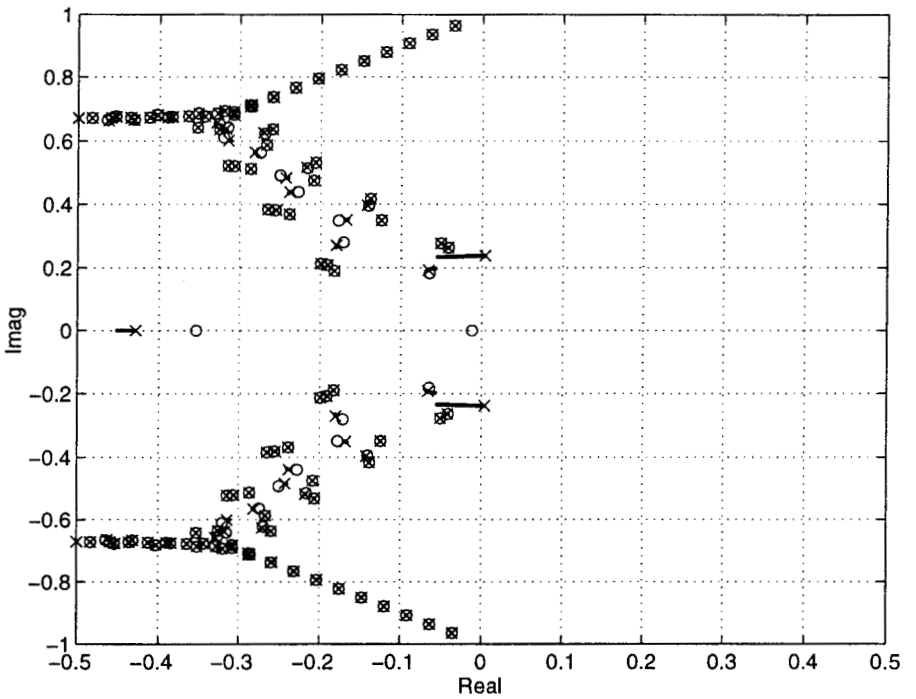

Figure 7: Root locus of optimal controller synthesized using Reduced-order Model in series with Validation Model plant for gain,K, varying from 0 to 4.

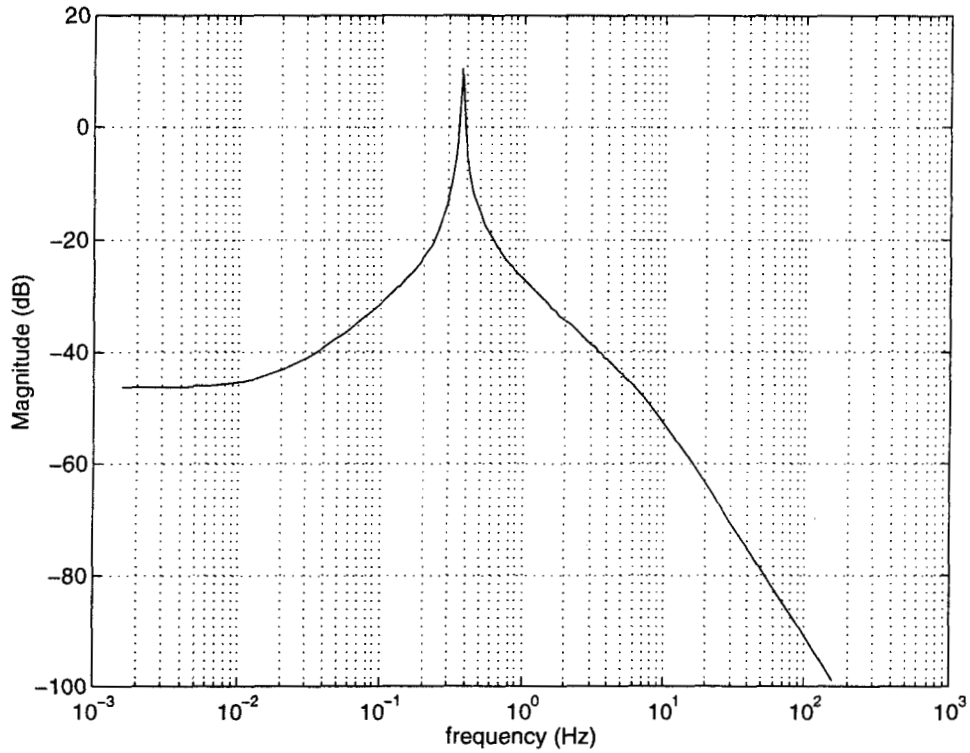

Figure 8: Open loop response magnitude for series connection of LQG controller (using Reduced-order Model) and Validation Model.

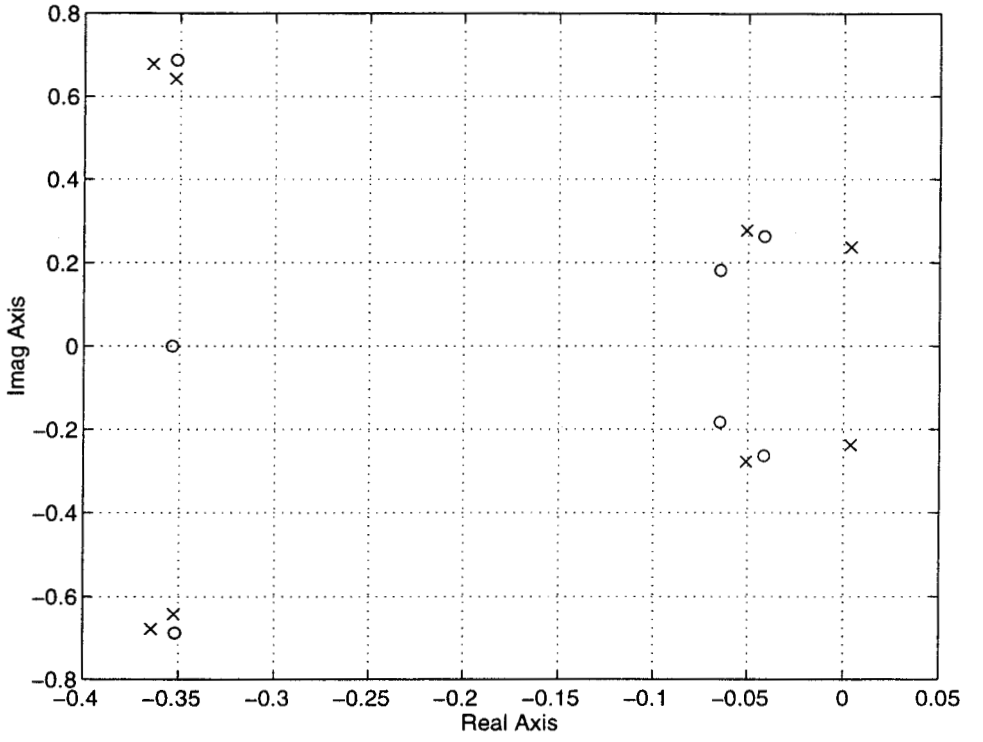

Figure 9: Pole (x) /Zero (o) configuration of Low-order Model.

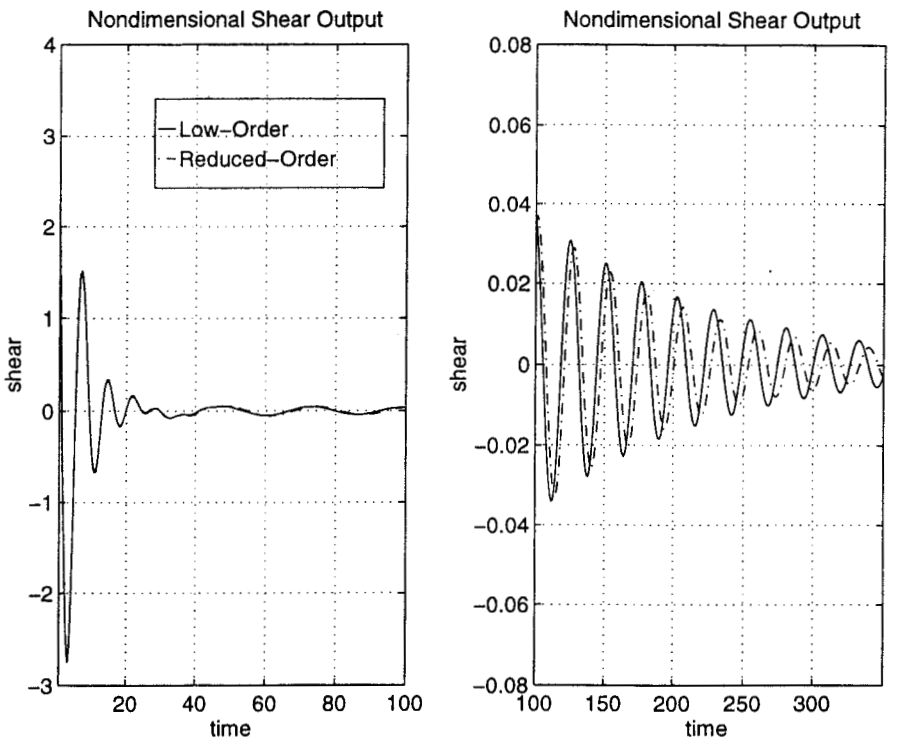

Figure 10: Dashed-dotted line is output from closed-loop system using reduced-order LQG controller. Solid line is output from closed-loop system using low-order LQG controller.